Motion mitigation in intensity modulated particle therapy by internal target volumes covering range changes

Christian Graeff,[a] Marco Durante, and Christoph Bert
GSI Helmholtzzentrum für Schwerionenforschung, 64291 Darmstadt, Germany

(Received 23 March 2012; revised 16 August 2012; accepted for publication 17 August 2012; published 14 September 2012)

Purpose: Particle therapy offers benefits over conventional photon therapy but also introduces sensitivity to changes in the water-equivalent path length (WEPL) in case of target motion, e.g., breathing. Target motion can be addressed by the internal target volume (ITV) approach, defined as the CTV plus target movement. In photon therapy, the ITV can be constructed as the geometric union of CTVs in all motion states (GEO-ITV) of a 4D-CT, but this does not account for WEPL-changes. An ITV including WEPL-changes can be defined as the union of all CTVs transformed to a WEPL-equivalent axis along beam's eye view. The resulting WEPL-ITV is field-specific and thus unsuitable for intensity modulated particle therapy (IMPT). The purpose of this study was an IMPT-compatible ITV by splitting geometrical motion and field-specific WEPL changes, following ICRU 78 recommendations.
Methods: For all fields, the GEO-ITV was used as a common target. This identical geometry for all fields was mapped to an enlarged WEPL extent with a field-specific transformation. As the dose distribution is determined by the WEPL, this is sufficient to achieve equivalent dose coverage as for a geometrically enlarged target volume. The WEPL enlargement is only visible to the specific field and therefore does not increase the target volume of other fields. This avoids unnecessary lateral field extensions, reducing the dose to normal tissue. Homogeneous dose coverage in IMPT is achieved only if the inhomogeneous doses from the individual fields match up during delivery. As the course of the WEPL within each motion phase differs, this cannot be guaranteed by optimizing the fields only in the reference phase. The WEPL-ITV for the reference phase can be amended by CTVs from a subset of motion phases (4D-WEPL-ITV). Here, end-exhale as the reference phase was combined with end-inhale to cover the whole motion range. The GEO-ITV, WEPL-ITV, and 4D-WEPL-ITV were applied in an IMPT simulation of a lung cancer patient case using a four-field geometry and the heart as an OAR. A static plan of the CTV in end-exhale was computed for reference. The CTV was moving approximately 20 mm in SI and was partly overlapping the heart. For a single fraction a target dose of 17.7 GyE was prescribed, with a 50% maximum dose for the heart.
Results: With 21 rescans to counter interplay, the homogeneity (D5-D95) was 17.0%, 9.0%, 6.0%, and 3.5% for the GEO-ITV, WEPL-ITV, 4D-WEPL-ITV, and a 3D CTV plan computed for reference, respectively. Due to the overlap, the 50% maximum dose was violated by all plans, with V50 of 3.8%, 3.5%, 3.7%, and 2.0% for the four plans.
Conclusions: A 4D-WEPL-ITV method was developed that is suitable for IMPT, covers range changes, and drastically improves dose homogeneity in the target without increasing the OAR dose.
 [http://dx.doi.org/10.1118/1.4749964]

Key words: particle therapy, radiotherapy planning, ITV, water-equivalent path length, organ motion, intensity modulation

I. INTRODUCTION

Particle therapy not only offers benefits over conventional photon therapy but also introduces sensitivity to the water-equivalent path length (WEPL) and its potential changes in case of a moving target such as a lung tumor. In addition, for scanned ion beams such as used at GSI, interplay effects between beam and target motion have to be compensated, e.g., by rescanning.[1]

A common approach to address target motion is the internal target volume (ITV), which expands the CTV to include motion.[2] In photon therapy, which is comparably insensitive to the WEPL, the ITV can be constructed by the geometric union of the target volume in all motion phases of a 4D-CT (GEO-ITV). The GEO-ITV is insufficient for particle therapy which is highly sensitive to WEPL.[3] Different strategies have been reported to include WEPL differences between motion phases both for passive and scanned beam delivery. A large part of the variation in the case of lung tumors results from the large density difference between solid tumor tissue and lung tissue. One option to reduce this effect is to replace low density values in the GEO-ITV by the average GTV value[4,5] or by some fixed HU value.[6] Additional margins compensate for range changes not covered by the modified CT.

Another ITV approach that covers range changes was proposed by Rietzel *et al.*[7] It is based on conversion of the target

to a WEPL coordinate system, i.e., geometric lengths are converted to WEPL along the beam central axis. The ITV is then constructed from the union of WEPL-converted CTVs from all motion phases of a 4D-CT. This union is converted back into a geometric volume in the reference phase to provide a target suitable for standard treatment planning routines. The WEPL-ITV is optimal in the sense that it covers the smallest additional volume necessary to compensate for WEPL-changes. In a recent study, Park *et al.* extended this concept to a clinically applicable technique that also includes setup uncertainties and their effect on the WEPL as well as uncertainties of the WEPL determination itself.[8] As these margins extend only in the BEV axis, they are field-specific. The direct application of these margins to the target volumes leads to different targets for each field. Thus this ITV concept is not compatible with intensity modulated particle therapy (IMPT). IMPT allows for considerably better OAR sparing,[9] which would also be desirable for moving targets.

The aim of this study was to provide a method for computing an ITV that both compensates range changes and permits IMPT, where inhomogeneous dose distributions of the individual fields typically lead to lower OAR doses. This was achieved by incorporating field-specific WEPL changes into the field characteristics instead of the common geometric target volume. Thus, field-specific WEPL changes are separated from other margins common to all fields, as recommended by the ICRU report 78.[10] The feasibility of this method is demonstrated for a lung cancer patient case.

II. MATERIALS AND METHODS

All methods were implemented in a 4D-extension of TRiP98, the treatment planning system for ion therapy developed at GSI.[11,12]

II.A. WEPL-ITV

The method originally proposed by Rietzel *et al.*[7] was implemented in TRiP98, where margins for WEPL changes are added to the targeted VOI. These new target volumes are necessarily field-specific. An alternative method using the same target volume for all fields is described in Sec. II.A.1. The two methods resulted in virtually identical plans for individually optimized fields. Due to the nonapplicability to IMPT, the approach of Rietzel *et al.* is not further elaborated in this study.

II.A.1. Field-independent WEPL-ITV

Figure 1 schematically illustrates the basic problem of correcting WEPL changes by adding margins directly to the target volumes. As these are field-specific, the margins for one field unnecessarily increase the target size for other fields, if a common target volume is desired (see Fig. 1, panel a).

In our approach, these margins are included into the field description itself, hiding them from all other fields. This is possible by changing the translation of the CT geometry into the WEPL specifically for each field. The standard conversion

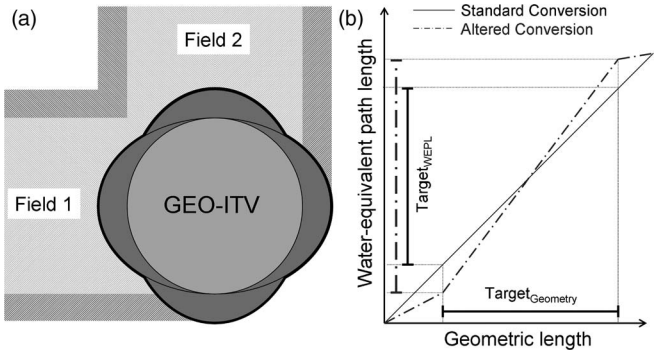

FIG. 1. Schematic depiction of the WEPL-ITV strategy. In panel a, a GEO-ITV (grey circle) is irradiated by two perpendicular fields. Both would require additional margins to cover for range changes in all motion phases, these are indicated as the two dark gray ellipses. The common target volume for both fields necessary to include all range margins is shown as the thick black contour. This would lead to an unnecessary lateral extension of both fields, as indicated by the dark gray striped entry channels. An alternative solution is depicted in panel b. Instead of using geometric margins, the same geometry is used for both fields, but the conversion of geometry to the WEPL is altered for each field. The graph in panel b depicts the standard conversion (solid line) for a central beam of one field passing the homogeneous CTV. An altered conversion (dashed-dotted line) increases the WEPL extent for the same geometry, resulting implicitly in the same effect as the geometric margin from panel a. This WEPL conversion hides the margins from other fields, so that both fields can use the minimal lateral extent (light gray entry channel).

given by the known HU-WEPL look-up table[13] is modified in such a way that the *same geometry* is converted to an *altered* WEPL extent. As the actual dose distribution in beam's eye view is determined by the WEPL and not by the geometric length, this is sufficient to achieve a target coverage equivalent to margins added directly to the target volume. An example of such an altered geometry-WEPL-conversion is given in Fig. 1, panel b. As indicated by the dashed-dotted line, this field-specific, new conversion now leads to a larger WEPL extent of the target corresponding to the one achieved by the margins added in Fig. 1, panel a.

This WEPL conversion is computed for each pencil beam position in each field. The aim of the altered conversion is to accumulate the WEPL extent of the target in all motion phases, following the concept of Rietzel and Bert.[7] To this end, the WEPL conversion is designed to extend from the minimum to the maximum WEPL value from all motion phases.

In case of multiple target or OAR intersections with the beam path, the necessary WEPL extent (minimum to maximum in all motion phases) is first computed for each of these sections individually. In a second step, overlapping sections are joined if they belong to the same structure. In case of conflicts between different structures, OARs are superseded by the target, i.e., their WEPL extent is shortened accordingly. In extreme cases, the WEPL extent of OAR structures can also be set to 0.

An example of the WEPL conversion is given in Fig. 2 for a lung tumor case (details in Sec. III.B.1). The graph shows the standard geometry-WEPL-conversion for all ten motion phases of the 4DCT. The conversions for end-exhale and

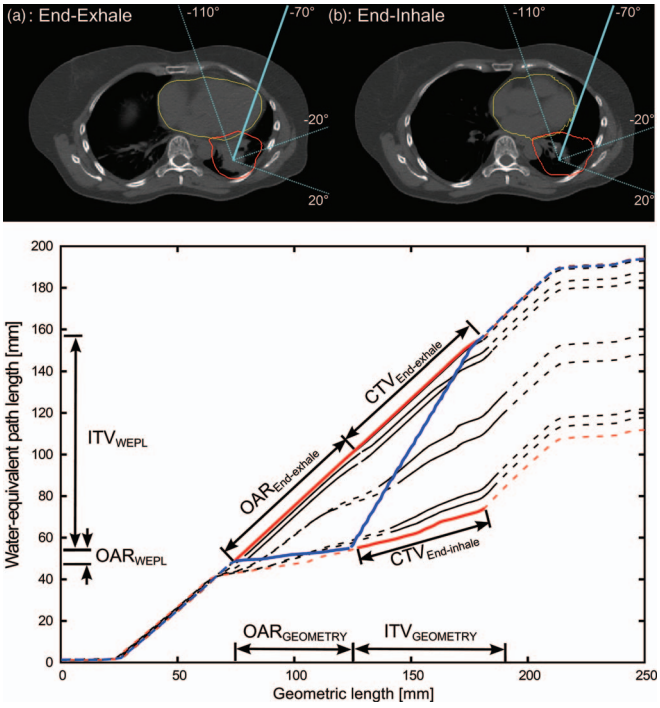

FIG. 2. Transversal slices at end-exhale (panel a) and end-inhale (panel b) of the lung cancer patient showing the contours of the CTV (red) and heart (yellow). The blue lines illustrate the four fields. In the graph, the WEPL-geometry conversion for the bold line of the –70° field is plotted for all motion phases, with end-exhale and end-inhale in red. Intersected volumes are printed solid. While in end-exhale the beam traverses nearly homogeneous soft tissue, the same beam in end-inhale passes through 100 mm of lung tissue, resulting in a considerably lower WEPL. The blue line shows the altered WEPL conversion, the extent for the OAR and target are indicated near the respective axes. The WEPL of the OAR overlapped with the target and was thus shortened.

end-inhale are shown in red, the corresponding beam paths are indicated as the bold lines in the transversal slices. In end-exhale, the central beam passes through homogeneous soft-tissue in both the OAR and the CTV, while the same point in end-inhale does not pass through the heart, but rather through lung tissue before entering the target. The target itself also consists mostly of lung tissue as the solid tumor has moved vertically out of the slice. Thus, the WEPL values for end-inhale are considerably lower than for end-exhale, as shown in the two red curves in Fig. 2.

The final WEPL conversion for this beam position is shown as the blue line, with target and OAR sections as solid lines. Due to the different WEPL curves in the motion phases, the CTV WEPL extent is greatly expanded compared to the extent of an individual motion phase, replacing the OAR and reducing it to a small WEPL extent.

The WEPL conversion is not unique, as specific values for the WEPL are only fixed for the borders of all target and OAR sections, but not for the transition within or between borders. These transitions differ between motion phases, so that no common values can be uniquely identified. The transformation is implemented as a mapping of the course of the WEPL in the reference phase to the maximal and minimal WEPL values required. An alternative could have been the average of all motion phases in which the beam intersects the currently investigated target. This approach would lead to frequent jumps in the WEPL unions when the number of contributing phases changes and was thus not used.

The common target volume for all fields is the GEO-ITV. The altered WEPL conversion modifies the targeted structure in the WEPL coordinate system independently for each field. This allows complete target coverage equivalent to the modified target volumes as originally defined by Rietzel and Bert.[7] The lateral extent of each field remains minimal, as it is not influenced by the WEPL margins from other fields.

II.A.2. The WEPL-ITV in IMPT

The inhomogeneous dose distributions of single fields resulting from IMPT require additional measures in optimization. The standard, 3D optimization method provides uniform dose coverage for the WEPL-ITV in the reference phase of the 4DCT. In case of IMPT, the inhomogeneous dose distributions of all fields have to match exactly to achieve a homogeneous target dose. When the optimization is performed for the reference phase only, the dose distributions do not necessarily fit together in other motion phases. This is caused by the different WEPL through different tissues in each of the motion phases. Even if the WEPL-ITV provides the correct minimum and maximum WEPL values, it can only represent a single slope in between these values. This slope of the WEPL will influence the actual distribution of the dose of each field, though.

This is illustrated in Fig. 3 for two schematic fields optimized for a simple square target with a given WEPL in a reference phase. The dose distributions of the two fields no longer complement in a motion phase where the target shows a lower radiological density. The reduction in density could

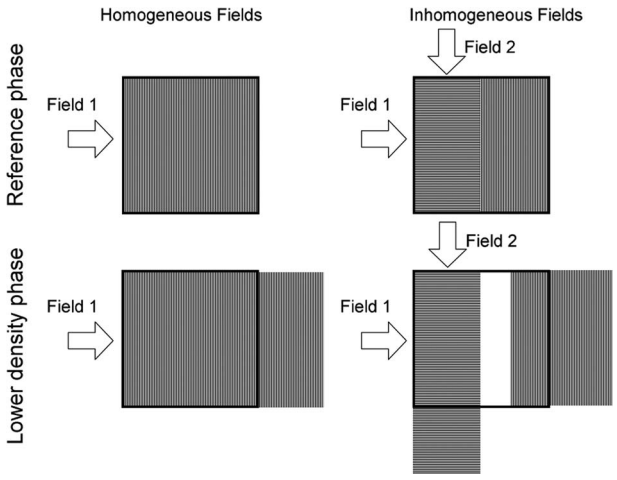

FIG. 3. Schematic depiction of the effect of homogeneous and inhomogeneous dose distributions from fields optimized in a reference phase (top row). Depicted is the area of target dose delivery. The same fields are then applied to another motion phase with a lower WEPL in the CTV only. This leads to an overshoot, but still good dose coverage for fields with homogeneous dose distribution (left column). The same overshoot leads to underdose for fields with inhomogeneous dose distributions that no longer match up in the nonreference phase.

be caused by a moving lung tumor, which in an identical transversal plane is replaced by less dense lung tissue for certain motion phases (see Fig. 2, panels a and b). This would not lead to a change in the WEPL-ITV, as the ranges in the nonreference phase are all within the limits of the reference phase, i.e., the borders of the WEPL-sections do not change. Still, the lower WEPL in the nonreference phase leads to an overshoot of both fields. Fields with homogeneous dose distributions achieve adequate dose coverage (Fig. 3, left), but inhomogeneous dose distributions in this case result in severe underdose (Fig. 3, right). An overdose can also be produced by analogous mechanisms. One solution to this problem is 4D-optimization which can take into account different motion phases and their different WEPL slopes.

It should be noted that this effect will in general not be observed in water phantom experiments or simulations, where the WEPL in front of and within the target is usually homogeneous throughout all motion phases. It will occur in the complex anatomy of patients, though.

To demonstrate this effect also in the patient study, both GEO-ITV and WEPL-ITV are also computed without constraints for the OAR, resulting in homogeneous fields. These should result in good dose coverage in case of the WEPL-ITV.

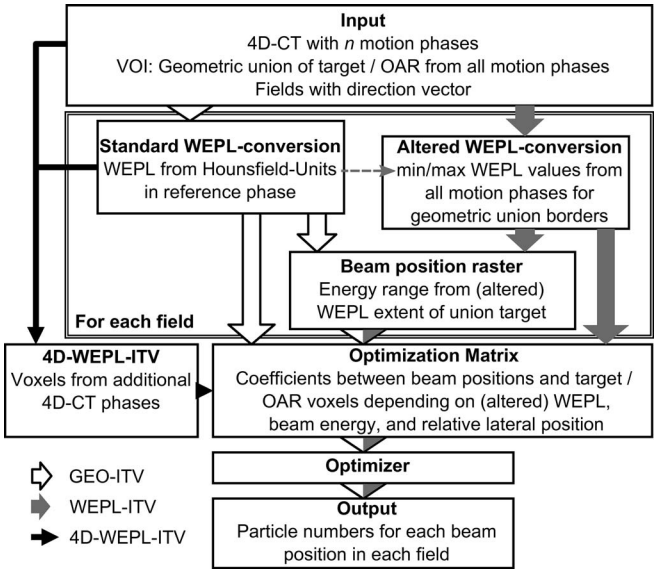

FIG. 4. Flow chart of the optimization process for GEO-ITV, WEPL-ITV, and 4D-WEPL-ITV. 4D-WEPL-ITV uses also the path of the WEPL-ITV. The three approaches basically differ in the way the optimization matrix is constructed; the input, the optimizer, and the output are identical. The altered WEPL affects the energy range of the initial beam spot raster, as well as the relationship between target/OAR voxels and beam spots.

II.A.3. 4D-optimization

The optimization of the biological dose corresponds to minimizing the residual of a nonlinear equation system.[13] In TRiP98, the optimization is computed by conjugate gradient algorithms. The following objective function describes the optimization for the physical dose:

$$E(\vec{N}) = \sum_{i\in\text{target}} \left(D^i_{\text{pre}} - D^i_{\text{act}}(\vec{N})\right) = \sum_{i\in\text{target}} \left(D^i_{\text{pre}} - \sum_{j=1}^{n} c_{ij} N_j\right). \quad (1)$$

With D_{pre} the prescribed and D_{act} the actual dose at a given CT voxel i. The coefficient c_{ij} describes the dose deposition of a beam position j at a voxel i, which depends among other factors on the WEPL. The number of particles N_j of each beam position from all fields is to be optimized. For full complexity, D_{act} is replaced by the expression for the biological dose and OAR constraints are included. The dose in OAR voxels is only evaluated in the objective function if it is larger than a given dose constraint, i.e., underdose in OARs is not considered. The objective function and additional terms for biological dose and OAR constraints do not change in the 4D formulation.

Figure 4 shows the workflow of the optimization process. The input determines the number and location of the target voxels, as well as their WEPL. The extent of the WEPL values determines the energy range of the beam position raster. For the WEPL-ITV, thus both the available beam positions and the WEPL-dependent coefficients c_{ij} differ from the GEO-ITV.

The number of raster points and the number of CT voxels are in the order of several 10 000. Most c_{ij} are small; and typically a threshold of 0.002 is applied to reduce the number of equations.

For the purpose of this study, the optimization needs to result into a single irradiation raster that is universally applicable to all motion phases, analogous to a standard ITV plan. The number of beam positions n and their geometric location thus remain unchanged. Instead, additional equations are included describing the dose deposition of each beam position to each target/OAR voxel *during specific motion phases*. It should be noted that the prescribed dose to each target voxel also does not change and is independent of the number of motion phases included in the optimization.

Two different 4D approaches are viable: The first one uses the above-introduced WEPL-ITV concept only to determine the necessary size of the set of beam positions that potentially has to be irradiated. For the actual optimization of the particle numbers N, the WEPL-ITV is no longer used. Instead the CTV of each motion phase k is included in the objective function, i.e., additional equations for each CTV voxel in each motion phase:

$$E(\vec{N}) = \sum_{k=1}^{m} \sum_{i\in\text{CTV}(k)} \left(D^i_{\text{pre}} - D^{ik}_{\text{act}}(\vec{N})\right) = \sum_{k=1}^{m} \sum_{i\in\text{CTV}(k)} \left(D^i_{\text{pre}} - \sum_{j=1}^{n} c_{ijk} N_j\right). \quad (2)$$

In this way, any possible target position is described by the correct, motion phase specific WEPL, obviating the need for an additional WEPL correction. The number of equations grows approximately by a factor of the number of motion states m, which might lead to inacceptable demands on

memory requirements and computation times. A practical use of this *4D-CTV* method could be a gating plan with a reduced number of motion states. An exemplary gating plan for a 30% window (end-exhale and 4D-CT adjacent phases) is computed using this approach.

An alternative would be to compute the WEPL-ITV for the reference phase and to include the CTV for a subset of additional phases $\underline{m}$ that are representative for the entire problem, e.g., end-inhale in addition to the reference phase end-exhale:

$$E(\vec{N}) = \sum_{i\in \mathrm{ITV}} \left(D^{i}_{\mathrm{pre}} - D^{i,\mathrm{ref}}_{\mathrm{act}}(\vec{N})\right) + \sum_{k\in\underline{m}} \sum_{i\in \mathrm{CTV}(k)} \left(D^{i}_{\mathrm{pre}} - D^{ik}_{\mathrm{act}}(\vec{N})\right). \quad (3)$$

The entire WEPL range of the ITV, with the characteristics of the reference phase, is thus covered by the first summand of Eq. (3), while the specific characteristics of other phases are covered by the second one. A particle allocation minimizing Eq. (3) is thus sufficient to match fields with inhomogeneous dose distributions in several motion phases. This leads to a more modest increase of the optimization problem but incurs a residual error as some of the motion phases are neglected. This method is used here to compute a 4D-WEPL-ITV plan for the full motion range. The first summand of Eq. (3) is identical to the objective function of the WEPL-ITV. The 4D-WEPL-ITV thus uses the same path as the WEPL-ITV in Fig. 4, but in addition also the black path adding the additional voxels of other motion phases.

For this second approach, as not all motion phases are included, phases need to be chosen carefully. Assuming a Lujan-type breathing pattern,[14] the end-exhale phase will be similar to its adjacent phases, while movement around end-inhale is stronger. The WEPL-ITV should thus be calculated for end-exhale, which is more representative for a larger part of the breathing cycle.

Both methods increase the number of constraints for the optimization. Thus the overall quality of the plan could be reduced as different conflicting goals are included into the optimization. The first 4D optimization option includes up to ten slightly different equations for each voxel in each motion phase. This might lead to fields with nearly homogeneous dose distributions as the only viable solution, defeating the purpose of IMPT. This is not further investigated here but could be of interest for future studies.

The input as well as the conjugate gradient methods is the same for all three approaches as shown in Fig. 4. Not shown is the also identical forward dose calculation, which especially does not use the altered WEPL conversion.

II.B. Patient study

II.B.1. Patient characteristics

The methods were investigated in a lung cancer patient. GEO-ITV, WEPL-ITV, and 4D-WEPL-ITV plans were calculated for the whole motion range, and 4D-CTV and GEO-ITV plans for the three motion phases around end-exhale. The patient showed a tumor in the lower left lobe exhibiting large SI motion of around 20 mm between end-exhale and end-inhale. A 10-phase 4D-CT was provided by M. D. Anderson Cancer Center (MDACC), Houston, TX, including contours for the CTV and several OARs such as the heart. Contours were provided only for the end-exhale phase but were propagated to all other phases using a nonrigid registration by Plastimatch.[15] To facilitate this, the original polygonal contours were converted to a binary mask.

A four-field-treatment plan geometry following the methodology at the National Institute of Radiological Sciences, Chiba, Japan[16] was used, see Fig. 2. The target dose for a single fractionation scheme was set to 17.7 GyE, using the Local Effect Model IV to compute the biological dose.[17] For IMPT,[9] the heart was assigned a maximum tolerance dose of 50% of the CTV-target dose. The WEPL adaptation was applied also to the heart. For better comparison to a potential application in proton therapy with a constant RBE, also physical doses for the carbon fields were also computed, neglecting the RBE.

In scanned particle therapy of moving targets, the two independent motions of target and beam interact, leading to distinct interplay patterns.[1] Thus, the 4D-dose was computed with 21 slice-by-slice rescans for the ITV plans, which was sufficient to reduce interplay effects. For the gating plans, three rescans were used. The number of necessary rescans was not further investigated; also a lower number might be sufficient. The 4D-CT was assumed to represent ten motion phases of equal duration. A motion with 5 s period was simulated to determine the actual motion phase; the timing of the raster spot irradiations was derived from simulated extraction schemes mimicking the GSI synchrotron. The combination of motion and irradiation timing then determined the motion phase in which each raster spot is irradiated. The dose deposited by the raster spots to the CT voxels was computed in the corresponding CT phase. The dose was accumulated in the reference phase using the nonrigid registration.[12]

Also, the static dose was calculated for end-exhale and end-inhale as the most diverse phases of the breathing cycle. An ideal ITV plan should achieve complete CTV coverage in all motion phases; a prerequisite to the absence of motion monitoring during treatment delivery. Static dose calculations of individual phases can thus be used as a quality measure for an ITV plan.

II.B.2. Data analysis

The dose was evaluated as the volume receiving more than 95% (V95) and more than 107% (V107) of the target dose, representing under- and overdose, respectively. The homogeneity was given by the difference of the dose given to 5% and 95% of the volume (D5-D95). The dose to the OAR was characterized by the volume receiving more than 50% of the target dose (V50), the median dose applied to 50% of the volume (D50), and the area under the curve of the DVH (AUC). As the dose restriction of the OAR was set to 50% of the target dose, V50 should be 0 for an optimal plan. All doses are given relative to the target dose, all volumes relative to the volume of the CTV or the OAR as appropriate.

In addition, the conformity number CN (Ref. 18) is reported for the CTV characterizing both target coverage and out-of-target dose. The conformity can be expected to be worse for static dose calculation for ITV plans. When calculating the 4D-dose, the only part of the ITV that is completely covered by the target dose is the CTV. In contrast, at least in the reference phase, the entire ITV should receive the target dose, leading to a markedly higher 95% dose volume outside the CTV.

III. RESULTS

For the patient used in this study, the heart and CTV overlap. No special care was taken to resolve this; within TRiP98, a target supersedes the OAR in the optimization. Therefore, perfect dose conformity cannot be achieved for both OAR and target. A static computation of the CTV is given as the reference achievable result (see Fig. 7(a) and Table II).

III.A. Changes in WEPL

An estimate of the differences in WEPL between the motion phases can be gained from the minimum and maximum WEPL observed by each field for either GEO-ITV or WEPL-ITV. As stated in Table I, the GEO-ITV both over- and underestimates the minimum and maximum WEPL necessary to cover the CTV in all motion phases. The pattern of changes is quite complex and can exceed 30 mm. For example, Field 1 has a considerably larger range of WEPL values in the GEO-ITV, with both a too small minimum and a too large maximum. In Field 4, the minimum is drastically overestimated, so that a large part of the target is not covered adequately.

It should be noted that the WEPL in Table I are computed from the extent of the entire target, and will thus partially mask differences between individual raster spot positions.

The large differences result from the strong SI movement of the tumor, so that solid tumor or liver tissue in the reference end-exhale phase are replaced by low-density lung tissue in end-inhale and vice versa.

III.B. Dose calculations

III.B.1. Target coverage

Ideally, an ITV plan should achieve CTV coverage in every motion phase. Thus, static dose calculations for the three ITV plans are shown for the extreme motion phases end-exhale (reference) and end-inhale in Fig. 5, with corresponding DVHs in Fig. 6. For the GEO-ITV, the dose coverage of the reference phase is sufficient; in end-inhale, though, it shows severe under- and overdoses resulting from both neglected water range and the fields with inhomogeneous dose distributions. The WEPL-ITV compensates for the change of the range extent, but does not match the specific range variations of individual Bragg peak positions within this extent for any phase. It thus shows lower but acceptable dose coverage for end-exhale; see also the DVH in Fig. 6. The dose coverage of end-inhale is improved in comparison to the GEO-ITV, but as it cannot match the inhomogeneous dose distributions of the single fields to the specific WEPL variations of the end-inhale phase, overdose still occurs.

The 4D-WEPL-ITV approach greatly improves the dose distribution in the end-inhale phase, to the point that it exceeds coverage in the reference phase in static calculation. This is a result of the end-inhale CTV included both directly and also as part of the WEPL-ITV.

In contrast, if the OAR was not considered in the optimization, the dose distributions of the fields would be homogeneous, and the WEPL-ITV is sufficient to achieve target coverage also for the moving target, see Table II. The GEO-ITV

TABLE I. Water-equivalent path lengths of the GEO-ITV and WEPL-ITV as used to calculate the necessary irradiation raster to cover the entire target volume.

	GEO-ITV WEPL (mm)			WEPL-ITV WEPL (mm)		
Field	Minimum	Maximum	Range	Minimum	Maximum	Range
Field 1 (–20°)	37.3	128.9	91.6	49.5	117.7	68.2
Field 2 (+20°)	54.4	128.8	74.4	44.8	128.7	83.9
Field 3 (+70°)	63.3	156.1	92.8	54.9	157	102.1
Field 4 (+110°)	93.5	174.7	81.2	58.1	175.4	117.3

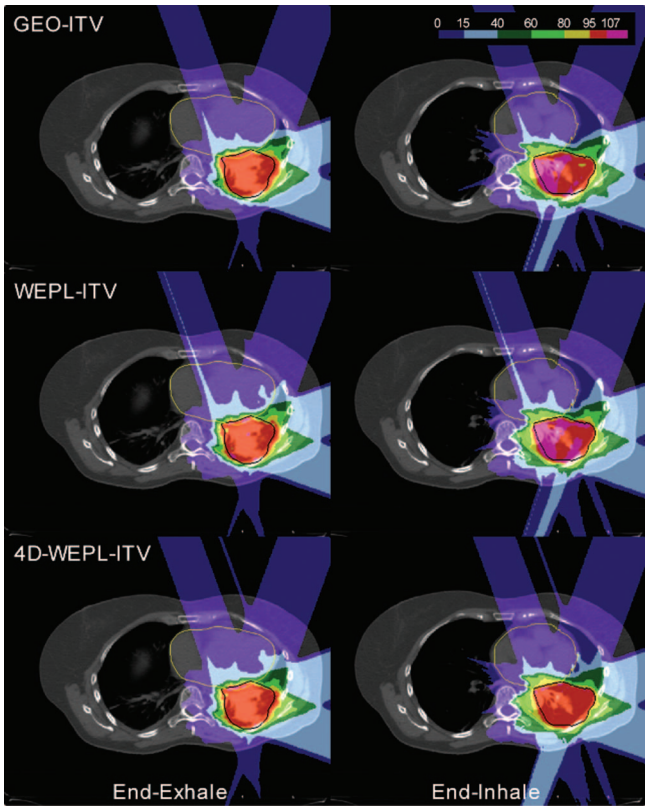

FIG. 5. Transversal, static dose cuts from end-exhale (reference phase, left panels) and end-inhale (right panels) with contours of heart (yellow) and CTV (black). All plans achieve dose coverage in reference, but in end-inhale, both GEO-ITV and WEPL-ITV cannot adjust for the inhomogeneous dose distributions of the single fields. The 4D-WEPL-ITV leads to a homogeneous dose from the sum of all fields in both phases. The color scale indicates percent of the prescribed dose.

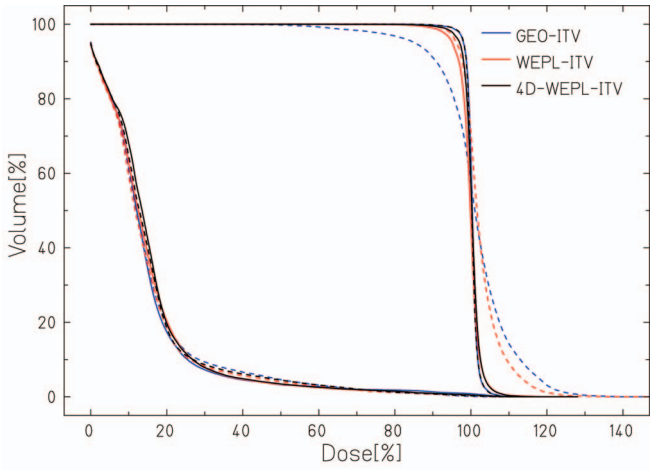

FIG. 6. DVH of the static dose calculation for the three ITV plans in both end-exhale (solid lines) and end-inhale (dashed lines). While the end-exhale phase dose coverage is acceptable for all plans, the end-inhale phase shows severe under- and overdoses, except for the 4D-WEPL-ITV.

still suffers from the neglected range changes and thus results in underdose, with V95 = 92.5%.

The dynamic dose coverage as it would be delivered assuming a regular breathing motion is shown in Fig. 7, for the GEO-ITV (panel b), the WEPL-ITV (panel c), and the 4D-WEPL-ITV (panel d). The impact of the individual phases on the dynamic dose is not equal. Due to the lower movement speed in end-exhale than in end-inhale, end-exhale is more similar to its neighboring motion phases. Thus it represents a larger part of the breathing cycle, influencing the delivered dose more. Also, some of the overdose in the non-reference phases averages out over the whole breathing cycle, so that, e.g., the dose coverage V95 of the 4D-dose for the

TABLE II. Results for the computed plans shown as V95 (underdose), V107 (overdose), and D5-D95 (homogeneity). All results are given in % of the target dose or the VOI size, respectively. The top row (static dose to the CTV in reference phase) serves as the reference dose distribution possible when the OAR is included into the optimization.

		CTV				OAR	
Target	Mode	V95	V107	D5-D95	CN	V50	D50
CTV	Static end-exhale	98.4	0.0	3.5	92.0	2.0	11.8
GEO-ITV	Moving	91.1	8.7	17.0	68.1	3.8	12.4
GEO-ITV	Static end-inhale	81.9	21.6	32.6	53.0	4.6	12.0
GEO-ITV	Static end-exhale	99.1	0.5	4.6	58.8	3.3	12.1
WEPL-ITV	Moving	98.7	3.8	9.0	78.0	3.5	12.6
WEPL-ITV	Static end-inhale	97.3	15.5	17.2	64.5	4.0	11.7
WEPL-ITV	Static end-exhale	95.3	1.2	8.6	67.7	3.3	12.5
4D-WEPL-ITV	Moving	99.3	0.3	6.0	78.3	3.7	13.6
4D-WEPL-ITV	Static end-inhale	99.1	0.3	4.7	66.9	4.5	12.8
4D-WEPL-ITV	Static end-exhale	98.0	1.1	6.7	68.1	3.4	13.5
GEO-ITV	Moving—no OAR	92.5	3.6	13.7	67.3	6.6	18.5
WEPL-ITV	Moving—no OAR	99.9	1.3	7.9	76.4	6.5	18.5
GEO-ITV	Gating 30%	96.5	1.1	8.0	88.8	2.1	11.2
4D-CTV	Gating 30%	97.7	0.6	6.8	90.1	2.2	11.8

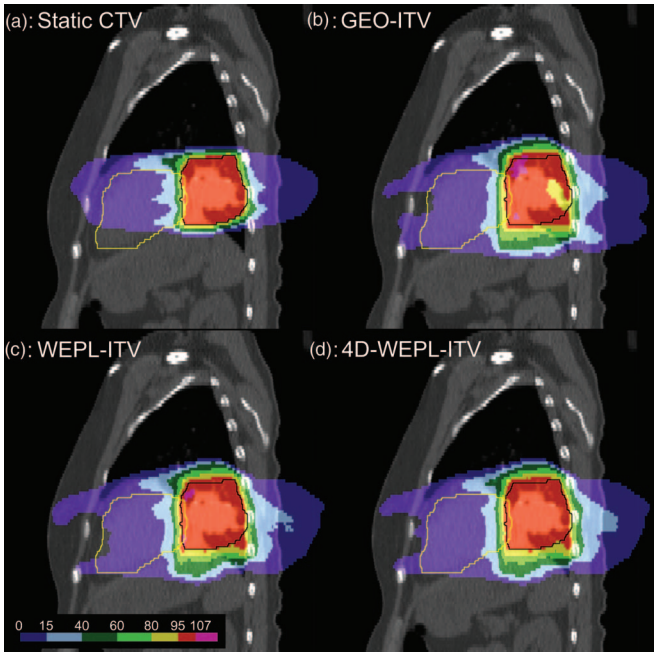

FIG. 7. Sagittal dose cuts for plans optimized for the static CTV (panel a) as a reference, and the 4D-doses for the GEO-ITV (b), the WEPL-ITV (c), and the 4D-WEPL-ITV (d) with contours of heart (yellow) and CTV (black). The WEPL-ITV offers a drastic improvement in dose coverage over the GEO-ITV, but the inhomogeneous dose distributions of the single fields in IMPT achieve adequate dose coverage only in 4D-optimization. The color scale indicates percent of the prescribed dose.

WEPL-ITV is higher than in the static reference phase, see Table II. The differences between the three ITVs are therefore not as large in the 4D-dose as in the static end-inhale dose.

The GEO-ITV showed both under- and overdoses, with V95 at 91.1% and V107 at 8.7%. The WEPL-ITV reduced the underdose considerably to the level of the static CTV reference, but incurred some overdose (V107 = 3.8%) due to the effect of inhomogeneous dose distributions of the single fields. The 4D-WEPL-ITV further improved the dose coverage and reduced the overdose to V107 = 0.3%. The homogeneity (D5-D95) is improved from 17.0% in the GEO-ITV to 9.0% in the WEPL-ITV, and 6.0% in the 4D-WEPL-ITV. The DVHs for the 4D-doses for all three ITV plans are given in Fig. 8.

The 4D-WEPL-ITV V95 actually exceeded that of the static CTV plan. This was a result of the enlarged ITV target, which replaced the OAR in the WEPL-union. Therefore, the conflict with the OAR in the optimization for the 4D-WEPL-ITV plan was lower than for the static CTV in end-exhale only.

All plans were also optimized for a physical dose without considering the RBE. In this case, the homogeneity D5-D95 was 19.9%, 12.3%, and 6.3% for GEO-ITV, WEPL-ITV, and 4D-WEPL-ITV, respectively. In comparison to the biological dose, there was a negligible change for the 4D-WEPL-ITV, but slightly more underdose and considerably more overdose for both WEPL-ITV and GEO-ITV. The doses to the OAR did not change notably.

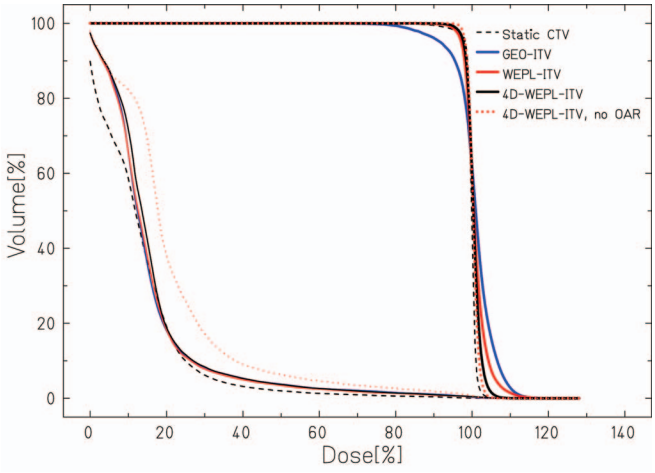

FIG. 8. DVH of the 4D-dose to the CTV (bold lines) and the OAR for the three ITV plans. The static CTV reference plan is shown as dashed lines. A plan neglecting the OAR is shown as the dotted lines, with considerably higher dose to the OAR.

III.B.2. Organ at risk sparing

The OAR tolerance dose of 50% of the target dose could not be met due to the overlap of the CTV. In the reference CTV optimization, V50 was 2.0%. All three ITV plans that included the OAR in the optimization resulted in a V50 of around 3.7%, nearly twice as high as the static reference. In contrast, the plans not including the OAR in the optimization showed a V50 of around 6.5%, so IMPT offered a major improvement.

The dose to the OAR remains unchanged between GEO-ITV, WEPL-ITV, and 4D-WEPL-ITV in spite of the improved target coverage, see Fig. 8 and Table II.

A major drawback of the ITV concept in general is the increased irradiation of healthy tissue. This is visible in Fig. 7, where all ITV plans result in an enlarged irradiated area mainly in SI direction. The reference CTV plan shows a conformity number CN of 92%, which cannot be met by the ITV plans. Still the CN is improved from 68.1% for the GEO-ITV to 78.0% for the WEPL-ITV and 78.3% for the 4D-WEPL-ITV. The reason for this is again the better matching of the water ranges over the whole breathing cycle. The CN also contains V95 as a factor, which only partially explains the lower result for the GEO-ITV.

III.B.3. Gating study

The gating plan calculated for the three motion phases around end-exhale shows a considerably lower homogeneity in comparison to the static reference, with respect to the small motion of only 1.3 ± 0.4 mm within the CTV.

The 4D-CTV results in slightly better dose coverage than the GEO-ITV (97.7% vs 96.5%, Table II). The OAR doses for both gating plans are comparable and not elevated from the static CTV reference. As can be expected the conformity number of the gating plans is higher than for the ITV plans as the residual motion and therefore also the irradiated volume is smaller. Again, the 4D-CTV performs slightly better than the GEO-ITV (90.1% vs 88.8%).

IV. DISCUSSION

In summary, we developed a method to compute an ITV that compensates for both target motion and range changes caused by motion. The method results in a target volume independent of beam directions compatible to IMPT. It allows for OAR-sparing dose distributions of the single fields by including multiple motion phases into the optimization process. The method showed clear benefits in target coverage and reduced dose to an OAR in a lung cancer patient case.

Compared to other approaches that use uniform margins to deal with range changes, the proposed method decreases the dose to normal tissue. As the distal margins necessary for range compensation due to organ motion are implicitly included in the field computation, this distal margin does not increase the irradiated volume for other fields. Distal margins added to the target volume geometry will show up as lateral margins for other, not directly opposed fields. As such, they necessarily increase the dose to healthy tissue, which can be avoided with the implicit approach chosen here.

The split of the ITV margins into a general part (the geometric union) and a field-specific part (the modified WEPL) is directly in line with the ICRU 78, where "adjustments ... within the beam-design algorithm"[10] are demanded to compensate for range uncertainties. Uncertainties common to all fields can then be included in the general definition of the PTV.

If fields are optimized individually, field-specific margins are acceptable. In this case, the method proposed by Park *et al.*[8] is sufficient for dose coverage in the presence of range changes. This approach also already includes additional margins for uncertainties not considered in this study, which is closer to clinical reality. Still, IMPT offers benefits in OAR sparing that are hard to achieve by single field optimization.

As stated above, the altered WEPL conversion is not unique. Potentially, a better choice of the conversion function could be more representative for all motion phases and thus minimize the necessity of 4D-optimization. The chosen approach uses an altered WEPL conversion based on the reference phase and is thus most representative for this phase. As stated above, the end-exhale phase is more similar to a larger part of the breathing cycle than any other phase, so that this choice appears reasonable. Still, a different function might be better suited for fields with inhomogeneous dose distributions. This remains to be investigated in future studies.

In this feasibility study, the robustness of the plan was not considered which is a crucial aspect especially for IMPT treatment plans. Only the motion as given by the 4D-CT and the resulting WEPL changes were used to compute the various ITV designs. For a clinically valid plan, additional margins as typically included in the PTV have to be applied. The altered WEPL conversion can readily be expanded to also include uncertainties in the range estimation, so that the separation of field-specific margins for range and margins common to all fields remains possible.

The size of field-specific margins needs to be investigated in further robustness studies. An upper limit is likely the 3 mm proximal and distal margins used in the ITV concept of

Koto *et al.*, which is in clinical use since several years.[4] Also, the sequence of the application of lateral and distal margin with respect to range adaptation needs to be investigated. For example, instead of the CTV as in this study, a "lateral PTV" could be used to compute the altered WEPL conversion. This would lead to a larger VOI but likely to better robustness than adding lateral margins to the WEPL-ITV. As the WEPL conversion incorporates range uncertainties, the margin typically added to the CTV likely can be reduced, but this also needs further studies.

Another possibility is a combination with optimization algorithms accounting for range uncertainties as proposed by Unkelbach *et al.*[19] Motion specific variations would be covered by the WEPL-ITV, while other range uncertainties would be incorporated in optimization. This would allow for a further separation of field-specific range uncertainties from other, field-independent sources of uncertainty.

In this study, a 4D-CT with equal duration of each motion phase was used, so that in all motion phases approximately the same number of raster spots is irradiated. For other 4D-CT methods with different durations of the different breathing phases, motion phases should be weighted accordingly during optimization to achieve good 4D-dose coverage.

We assumed a completely regular breathing pattern. The 4D-optimization leads to homogeneous dose distributions in the different motion phases so that irregular breathing patterns should not have a significant impact, as long as the breathing is represented by the 4D-CT. This was investigated in detail for IMRT.[20,21]

The patient study was mainly used to demonstrate the feasibility of our approach. The field geometry, with one of the fields traversing the heart, might not make sense in a real clinical setting. This field was retained to show the capabilities of IMPT to amplify fields for better OAR sparing. This also implies that the observed benefits will likely be smaller in a clinical setting with a more careful selection of field geometry, i.e., a lower degree of inhomogeneity in the fields. Still, the proposed algorithm allows for optimized OAR sparing in settings where OARs cannot be spared by field geometry alone, such as prostate cancer, where inter-fractional motion could be compensated.

In the patient study, the 4D-WEPL-ITV approach reduced underdose in comparison to the GEO-ITV and overdose in comparison to the WEPL-ITV optimized in a single phase only. The GEO-ITV did not compensate for errors either from range changes or from the mismatched dose distributions of the single fields, while the WEPL-ITV suffered only from the latter error. Additional simulations of fields with homogeneous dose distributions were computed to further investigate the size of the errors. The neglected range changes appeared to have a more severe impact, resulting in unacceptable underdoses. Further simulations with additional patients are necessary to quantify the size of the error, likely the clear division in under- and overdoses between the two error types is patient specific.

A general drawback of the ITV concept in combination with rescanning is the increased dose to normal tissue as a result of the enlarged target volume. In a recent study, Roland *et al.* propose a reduced size of the geometric ITV in photon therapy to reduce normal tissue irradiation.[22] The reduction was based on interpolating a volume between the union and the intersection of the CTVs from all motion phases, judged by the dosimetric effect. This concept could be incorporated into the WEPL-ITV, though the specifics of particle therapy, especially the range-dependency need to be considered. Still, the exemplary gating plans resulted in a higher dose conformity number, comparable to the static reference plan. In addition to gating, beam tracking might improve dose conformity. Both techniques require motion monitoring during treatment delivery though, which leads to a considerable higher degree of complexity.

The patient case was computed for the effective biological dose of carbon therapy, but the findings also held up for a physical dose without considering the RBE, where the misdosages for both GEO-ITV and WEPL-ITV were even worse. This indicates that the 4D-WEPL-ITV could also be useful for proton therapy, although the specific effects in proton therapy need to be studied further.

In conclusion, the 4D-WEPL-ITV permits intensity modulated particle therapy while also compensating range changes. By using field-intrinsic margins, the range compensation does not lead to lateral margins in other fields, sparing healthy tissue and maintaining a common target volume. In an exemplary patient study, the 4D-WEPL-ITV resulted in a highly conformal plan without increasing the dose to the OAR.

ACKNOWLEDGMENTS

The authors are grateful to Lei Dong, PhD, MDACC, Houston, TX, who provided 4D-CT data and contours for the lung cancer patient. The authors would like to thank John G. Eley for language editing. This research is in part funded by Siemens AG, Healthcare Sector, Imaging & Therapy Division, Particle Therapy, Erlangen, Germany. The authors report no conflicts of interest in conducting the research.

[a]Author to whom correspondence should be addressed. Electronic mail: c.graeff@gsi.de

[1]C. Bert and M. Durante , "Motion in radiotherapy: Particle therapy," Phys. Med. Biol. **56**, R113–R144 (2011).
[2]ICRU, "Prescribing, recording and reporting photon beam therapy," ICRU Report No. 62 (International Commission on Radiation Units and Measurements, Bethesda, MD, 1999).
[3]M. F. Moyers, D. W. Miller, D. A. Bush, and J. D. Slater, "Methodologies and tools for proton beam design for lung tumors," Int. J. Radiat. Oncol. Biol. Phys. **49**, 1429–1438 (2001).
[4]M. Koto, T. Miyamoto, N. Yamamoto, H. Nishimura, S. Yamada, and H. Tsujii, "Local control and recurrence of stage I non-small cell lung cancer after carbon ion radiotherapy," Radiother. Oncol. **71**, 147–156 (2004).
[5]T. Miyamoto *et al.*, "Curative treatment of Stage I non-small-cell lung cancer with carbon ion beams using a hypofractionated regimen," Int. J. Radiat. Oncol. Biol. Phys. **67**, 750–758 (2007).
[6]M. Engelsman, E. Rietzel, and H. M. Kooy, "Four-dimensional proton treatment planning for lung tumors," Int. J. Radiat. Oncol. Biol. Phys. **64**, 1589–1595 (2006).
[7]E. Rietzel and C. Bert, "Respiratory motion management in particle therapy," Med. Phys. **37**, 449–460 (2010).
[8]P. C. Park *et al.*, "A beam-specific planning target volume (PTV) design for proton therapy to account for setup and range uncertainties," Int. J. Radiat. Oncol. Biol. Phys. **82**, e329–e336 (2012).

[9]A. Gemmel, B. Hasch, M. Ellerbrock, W. K. Weyrather, and M. Kramer, "Biological dose optimization with multiple ion fields," Phys. Med. Biol. **53**, 6991–7012 (2008).
[10]ICRU, "ICRU Report 78: Prescribing, recording and reporting proton-beam therapy," J. ICRU **7**, 1–210 (2007).
[11]M. Krämer, O. Jäkel, T. Haberer, G. Kraft, D. Schardt, and U. Weber, "Treatment planning for heavy-ion radiotherapy: Physical beam model and dose optimization," Phys. Med. Biol. **45**, 3299–3317 (2000).
[12]C. Bert and E. Rietzel, "4D treatment planning for scanned ion beams," Radiat. Oncol. **2**, 24 (2007).
[13]M. Krämer and M. Scholz, "Treatment planning for heavy-ion radiotherapy: Calculation and optimization of biologically effective dose," Phys. Med. Biol. **45**, 3319–3330 (2000).
[14]A. E. Lujan, E. W. Larsen, J. M. Balter, and R. K. T. Haken, "A method for incorporating organ motion due to breathing into 3D dose calculations," Med. Phys. **26**, 715–720 (1999).
[15]J. A. Shackleford, N. Kandasamy, and G. C. Sharp, "On developing B-spline registration algorithms for multi-core processors," Phys. Med. Biol. **55**, 6329–6351 (2010).
[16]T. Miyamoto *et al.*, "Carbon ion radiotherapy for stage I non-small cell lung cancer," Radiother. Oncol. **66**, 127–140 (2003).
[17]T. Elsässer *et al.*, "Quantification of the relative biological effectiveness for ion beam radiotherapy: Direct experimental comparison of proton and carbon ion beams and a novel approach for treatment planning," Int. J. Radiat. Oncol. Biol. Phys. **78**, 1177–1183 (2010).
[18]A. van't Riet, A. C. Mak, M. A. Moerland, L. H. Elders, and W. van der Zee, "A conformation number to quantify the degree of conformality in brachytherapy and external beam irradiation: Application to the prostate," Int. J. Radiat. Oncol. Biol. Phys. **37**, 731–736 (1997).
[19]J. Unkelbach, T. C. Chan, and T. Bortfeld, "Accounting for range uncertainties in the optimization of intensity modulated proton therapy," Phys. Med. Biol. **52**, 2755–2773 (2007).
[20]A. Trofimov *et al.*, "Temporo-spatial IMRT optimization: Concepts, implementation and initial results," Phys. Med. Biol. **50**, 2779–2798 (2005).
[21]O. Nohadani, J. Seco, and T. Bortfeld, "Motion management with phase-adapted 4D-optimization," Phys. Med. Biol. **55**, 5189–5202 (2010).
[22]T. Roland, R. Hales, T. McNutt, J. Wong, P. Simari, and E. Tryggestad, "A method for deriving a 4D-interpolated balanced planning target for mobile tumor radiotherapy," Med. Phys. **39**, 195–205 (2012).